# The first billion years according to JWST

Adamo, A.; Atek, H.; Bagley, M.B.; Bañados, E.; Barrow, K.S.S.; Berg, D.A.; ... ; Nota, A.

nature astronomy

Perspective

https://doi.org/10.1038/s41550-025-02624-5

# The first billion years according to JWST

Received: 12 June 2024

Accepted: 16 June 2025

Published online: 8 August 2025

Check for updates

**Angela Adamo [1], Hakim Atek [2], Micaela B. Bagley [3], Eduardo Bañados [4], Kirk S. S. Barrow [5], Danielle A. Berg [3], Rachel Bezanson [6], Maruša Bradač [7,8], Gabriel Brammer [9,10], Adam C. Carnall [11], John Chisholm [3], Dan Coe [12,13,14], Pratika Dayal [15], Daniel J. Eisenstein [16], Jan J. Eldridge [17], Andrea Ferrara [18], Seiji Fujimoto [3], Anna de Graaff [4], Melanie Habouzit [4], Taylor A. Hutchison [19], Jeyhan S. Kartaltepe [20], Susan A. Kassin [12,14], Mariska Kriek [21], Ivo Labbé [22], Roberto Maiolino [23,24,25], Rui Marques-Chaves [26], Michael V. Maseda [27], Charlotte Mason [9,10], Jorryt Matthee [28], Kristen B. W. McQuinn [12,29], Georges Meynet [26], Rohan P. Naidu [30], Pascal A. Oesch [9,10,26], Laura Pentericci [31], Pablo G. Pérez-González [32], Jane R. Rigby [19], Guido Roberts-Borsani [26], Daniel Schaerer [26], Alice E. Shapley [33], Daniel P. Stark [34], Massimo Stiavelli [12], Allison L. Strom [35,36], Eros Vanzella [37], Feige Wang [38,39], Stephen M. Wilkins [40,41], Christina C. Williams [42], Chris J. Willott [43], Dominika Wylezalek [44] & Antonella Nota [12,45]** ✉

With stunning clarity, the JWST has revealed the Universe's first billion years. The scientific community is analysing a wealth of JWST imaging and spectroscopic data from that era, and is in the process of rewriting the astronomy textbooks. Here, as a result of the 2024 ISSI Breakthrough Workshop, we provide a snapshot of the great progress made towards understanding the initial chapters of our cosmic history 1.5 years into the JWST science mission. We present the current census of early galaxies, their luminosities, appearance, chemical composition, masses and formation histories as revealed by JWST. We relate the discovery of massive black holes in early galaxies and discuss their demographics and implications for their formations and growth. We conclude by describing the potential sources of reionization and our current understanding of how the Universe became fully ionized. Throughout the Perspective, we highlight discoveries and breakthroughs, topics and issues that are not yet understood, and questions that will be addressed in the coming years, as JWST continues its revolutionary observations of the early Universe.

The first billion years of cosmic history were the most eventful, rich with firsts and transformations (see a graphic representation in Fig. 1). After the Big Bang and initial accelerated expansion, the Universe's temperature and density constantly declined until photons and matter decoupled, initiating a period known as the cosmic 'dark ages'. It is during this period that the seeds leading to the formation of the first stars and primordial galaxies were growing. Slow perturbations of dark matter accreted baryons until the conditions for the ignition of the first stars were met; the very first sources of light in the Universe. The energy, momentum and enriched material ejected by these stars initiated the sparks that would eventually lead to the last major phase transition of matter, the epoch of reionization, consisting of the ionization of the neutral hydrogen permeating the Universe. This time of infancy for galaxies, where star-formation processes and black hole (BH) formation and growth take place, is fundamental for our understanding of galaxy growth and evolution. Unfortunately,

A full list of affiliations appears at the end of the paper. ✉e-mail: antonella.nota@issibern.ch

https://doi.org/10.1038/s41550-025-02624-5

we know the least about this early time—many questions remain about the basic facts and chronology.

When did the first stars form? Were they very different from the stars today? When did stars and gas coalesce to form the first galaxies? What did they look like? Did any early galaxies have disks like our Milky Way, or were they disordered and bursting with star formation? When did the first supermassive BHs form and fuel active galactic nuclei (AGN) powerful enough to impact the star formation of entire galaxies? How quickly did supernovae enrich their surroundings with heavy elements and dust, the building blocks of planets and life? And what was the timeline and topology of the last major phase transition of the Universe, as light steadily reionized the hydrogen gas permeating the Universe?

The James Webb Space telescope (JWST) is now enabling us to address these questions with direct observations of the light of these early galaxies emitted more than 13 billion years ago and redshifted into the infrared by the expansion of the Universe. This is the first and overarching success that JWST has unlocked: that it is possible to do these studies at all. With 10 times better resolution and a 100 times greater sensitivity than previous telescopes at similar wavelengths[1], JWST's four science instruments, the Near Infrared Camera (NIRCam), the Near Infrared Spectograph (NIRSpec), the Near Infrared Imager and Slitless Spectrograph (NIRISS) and the Mid-Infrared Instrument (MIRI) can complete in hours of observations what previously would have taken years, and therefore would have been unfeasible.

We refer to lookback time and distance in units of redshift ($z$), starting at $z = 5.6$, 1 billion years after the Big Bang according to standard cosmological models[2], and pushing back in time to the highest redshifts yet observed.

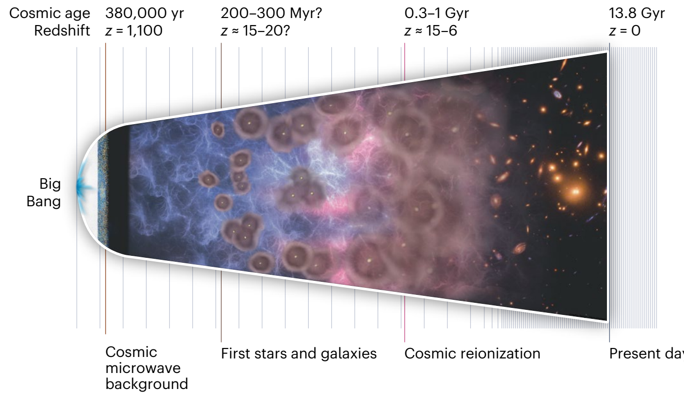


**Fig. 1 | The cosmic timeline.** The cosmic timeline from the origin of the Universe in the Big Bang, 13.8 billion years ago, until the present day. In the current standard picture, the Universe underwent a period of accelerated expansion called 'inflation' that expanded the Universe by about 60 orders of magnitude. The Universe then kept cooling and expanding until the next major epoch of 'recombination' about $4 \times 10^5$ yr later when the first hydrogen atoms formed. This was followed by the 'dark ages' of the Universe that lasted for a few hundred million years. The emergence of the earliest galaxies, a few hundred million years after the Big Bang, marked the start of the era of 'cosmic dawn'. The first galaxies also produced the first photons capable of ionizing the neutral hydrogen atoms permeating space, starting the epoch of reionization, the last major phase transition of matter in the Universe. In the initial stages of reionization, isolated galaxies (light yellow dots) produced ionized regions (grey patches) that grew and merged until the Universe was fully reionized. Credit: DELPHI project (ERC 717001). EU Research SPR19/P53.

## The physical properties of early galaxies

Before JWST, our view of distant galaxies was fundamentally simplistic—galaxies were unresolved, sources at the redshift frontier were mostly limited to extreme intrinsic luminosities, and star light and spectral features beyond the rest ultraviolet (UV) were largely out of reach. Using JWST, we have begun to chart a full census of the emerging and evolving population of distant galaxies, with a wealth of spatial and spectral information to pinpoint their distances, characterize their stellar growth and chemical enrichment histories, and resolve their complex structures and kinematics. In this section, we review these advancements.

### Extending the redshift frontier

JWST data reveal a robust population of high-redshift galaxies at $z > 10$, beyond the reach of the Hubble Space Telescope (HST; Fig. 2). In most cases, the galaxies are selected through the signature, in multi-colour imaging, of a sharp spectral cut-off bluewards of the Lyman-α line. This requires the galaxies to be reasonably luminous in the rest-frame UV. Many hundreds of such candidates have been identified at $z > 7$ (see next section and Fig. 2), and about 20 have been spectroscopically confirmed at $z > 10$ (refs. 3–11), with the current high mark at $z = 14.32$ (ref. 11). This record will surely not hold, as there is no technical limit on finding galaxies to $z = 20$.

### UV luminosity function

From these samples, JWST has produced a precise determination of the galaxy UV luminosity function and luminosity density (the integral of the luminosity function over a defined galaxy magnitude range), $\rho_{UV}(z)$, at redshifts $z \gtrsim 7$ (Fig. 2, and refs. 12–18, for example).

The UV luminosity function provides insight into the population of young, star-forming galaxies, offering constraints on their number density, luminosity and size. JWST's sensitivity in the near-infrared enables the detection of galaxies as far back as redshift $z > 10$, extending the study of galaxy formation to the epoch when the first galaxies emerged. High-redshift UV luminosity function measurements also help inform our understanding of cosmic reionization, the process that ended the 'cosmic dark ages' by ionizing hydrogen gas. Furthermore, the UV luminosity function provides essential data for testing cosmological models and assessing the effectiveness of observational techniques in probing distant, faint sources.

The decrease of $\rho_{UV}(z)$ is slower than generally expected before JWST, implying a more sustained early production of UV photons. Moreover, we observe that the bright end of the luminosity function does not significantly evolve between $8 < z < 12$ (refs. 19–23) due to an unexpectedly large number of luminous (where the absolute UV magnitude, $M_{UV} \approx -21$) galaxies with blue spectral slopes $\beta < -2$ (refs. 24,25). The abundances are still limited in precision due to detected field-to-field variation attributed to large-scale structure[18], but these findings have important implications for cosmic reionization as discussed in the 'Reionization' section.

Various physical scenarios, along with existing semi-analytic, semi-numerical models and simulations (for example, refs. 26,27), have been proposed to explain the evolution of the luminosity function. These include: (1) dust clearing by radiation-driven outflows[28,29]; (2) star-formation variability resulting in a flattening of the luminosity function[30–32]; (3) reduced feedback resulting in a higher star-formation efficiency[33,34]; and (4) a top-heavy initial mass function (IMF)[35], although see ref. 36. Although individual solutions (or more likely, a combination of) might provide a viable interpretation purely using astrophysical arguments, it cannot be excluded that modifications to the currently favoured $\Lambda$ cold dark matter model ($\Lambda$CDM; where $\Lambda$ is the cosmological constant) cosmology could also be required[37–39]. Thus, JWST data offer a unique tool to constrain and improve cosmological scenarios.

The faint end of the luminosity function is also important, as it depends on the nature of feedback processes acting in low-mass galaxies. Pre-JWST data suggested a steepening slope at higher redshift, but early JWST results appear to indicate a convergence to a logarithmic slope of $\alpha = -2$ in the luminosity function, suggesting that extremely faint galaxies dominate the cosmic star-formation rate density.

https://doi.org/10.1038/s41550-025-02624-5

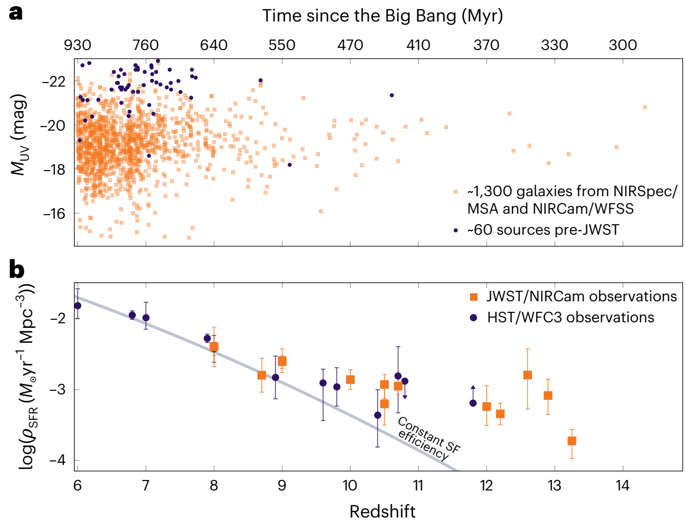


**Fig. 2 | JWST spectroscopic redshift compilation.** **a**, The distribution of absolute magnitudes and redshifts of spectroscopically confirmed galaxies from pre-JWST candidates (blue dots) and from public JWST datasets (orange squares), showing the power of JWST to detect galaxies beyond redshift 6. The latter include compilations[120] and single targets[10,11] observed with NIRSpec MSA observations, as well as NIRCam grism (First Reionization Epoch Spectroscopically Complete Observations (FRESCO)[179] and Emission-line galaxies and Intergalactic Gas in the Epoch of Reionization (EIGER)[128]). **b**, The cosmic SFR density over the first billion years as seen from HST/WFC3 samples (dark circles), compared with JWST/NIRCam estimates (light squares). A model of constant star-formation (SF) efficiency is plotted in grey, for comparison. The model and all literature points are derived from ref. 4 (and references therein), where the latter are integrated down to $M_{UV} = -18$ mag. The error bars are 1$\sigma$. SFR, star formation rate; WFC3, Wide Field Camera 3. Figure adapted from ref. 4 under a Creative Commons license CC BY 4.0.

## Stellar mass census

Massive stars produce most of the UV light but most of the mass in galaxies is emitted in the rest-frame optical and near-infrared. In contrast to HST, JWST's wavelength coverage and spectral sampling of the rest-frame optical thus allows tracking of the bulk of the stellar mass. These constraints are resolving earlier degeneracies regarding the contribution of emission lines, versus stellar continuum, enabling more accurate characterization of galaxy physical properties even beyond $z = 10$ when the rest-frame optical emission of galaxies redshifts into the MIRI wavelength range.

The rest-frame optical observations enable improved constraints on stellar mass, placing the first robust constraints on the rate of mass build-up in early galaxies, back to the first 500 Myr (refs. 40,41). Pre-JWST observations with HST, the Spitzer Space Telescope and the Atacama Large Millimeter/submillimeter Array (ALMA) had shown the potential existence of rare, massive and red galaxies beyond $z > 4$ that were typically excluded from rest-frame UV selections. JWST data reveal that these previously missed galaxies also contribute significantly to the stellar census[42,43]. An exciting frontier is access to the rest-frame infrared provided by MIRI. The inclusion of long-wavelength MIRI photometry extending out to 21 μm in the observed frame suggests a reduction in stellar mass estimates by typically 0.6 dex for massive ($\log(M/M_\odot) > 10$), red, dust-obscured sources at $z > 3$ (refs. 44,45). Accordingly, MIRI data are crucial to prevent overestimates of stellar mass in mature stellar populations at high redshift.

One compelling, although contentious, new population that emerged from the first JWST data was luminous and (overly) massive candidates at $z \gtrsim 6$ with redder-than-expected colours (for example, refs. 46,47). If interpreted correctly, these would require impossible or implausible star-formation efficiencies[48]. However, there has been significant debate within the community regarding how to incorporate the relative importance of star light, dust obscuration and actively accreting supermassive BHs when modelling the new datasets. So far, spectroscopic follow-up of many of the earliest ($z > 6$) massive candidates reveal strong emission lines due to star formation and/or AGN, which had been masquerading and/or exaggerating continuum breaks[49,50], hence alleviating the tension.

However, potential descendants suggest that the problem has not disappeared; a population of old and massive galaxies at later times ($z \approx 2$–$4$) also seems to require very efficient and rapid formation at $z \gtrsim 8$ (refs. 51–54). Such extreme formation efficiency still presents significant challenges for theoretical galaxy-formation models (for example, refs. 55,56). Larger spectroscopic samples, which enable more detailed stellar population modelling, will further test the extent of this tension.

Accurate characterization of the optical rest-frame emission also paves the way to probe the growth of galaxies and the structural and kinematics of their stars and gas, and to map star-formation sites and their feedback in terms of energy, momentum and metal enrichment injected in the galaxy medium, as discussed in detail below.

## Star-formation histories

Simulations of galaxy formation predict an early period of stochastic star formation at high redshifts and low masses; JWST is beginning to confront these predictions. Such stochasticity in early star-formation histories can be induced by various feedback processes, such as (1) photoevaporation of molecular hydrogen, (2) supernova explosions, and (3) cosmological accretion/merging, which dominate low-, intermediate- and high-mass systems, respectively, and act on different timescales[31,32,57]. Modelling the new imaging and spectroscopic data from JWST shows that $z > 6$ galaxies contain stars that are young, with typical inferred average ages of ~50 Myr, although younger (<10 Myr; for example, refs. 23,58–62) and older[63,64] samples exist. Rest-frame optical ([O III] + Hβ) emission-line equivalent-width distributions and UV slopes also indicate bursty star formation, with both on and off modes[65–67], also referred to in the literature as stochastic star formation episodes. In addition, spatially resolved data that isolate multiple stellar populations also emphasize that outshining can lead to significant stellar mass underestimates (up to 0.5 dex)[68–70]. Ultimately, as spectroscopic samples become more detailed and representative and analysis tools are optimized for the new datasets, we expect significant progress in obtaining robust galaxy stellar mass estimates.

## Structural and kinematic properties

The distribution (for example, size, morphology) of rest-optical light within galaxies, which traces all stars not just the youngest and biased O and B stars, and their internal kinematics reveals the overall efficiency and nature of the physical processes driving galaxy formation and evolution. The dramatic improvement in the spatial resolution and wavelength coverage of JWST's NIRCam instrument compared with its HST predecessors has enabled a sharper and more complete view of the distribution of stars in galaxies beyond $z \approx 7$. The rest-frame optical size–mass relation has been measured well beyond the previous limits—probing the mass distributions (not just youngest stars) for even dwarf-galaxy progenitors and pushing beyond cosmic noon ($z > 3$). These low-mass galaxies are more extended than conventional scaling relations would have predicted (for example, ref. 71). High-redshift galaxies at $z \gtrsim 7$ roughly extend earlier relations, more rapidly evolving for quiescent galaxies than their star-forming counterparts (for example, refs. 72–74).

The same NIRCam imaging yields an unparalleled view of the stellar structures of those same galaxies. Although galaxies at high redshift ($z > 3$) exhibit a broad diversity of morphologies, visual inspection has revealed that disk-like galaxies appear at early times (~60% at $z = 3$, 30% at $z \approx 6$–$9$; for example, refs. 75–78). These studies have included galaxies that were previously faint, or undetected in HST imaging (for example, ref. 79). Remarkably, the imaging also enables the identification of more detailed structures, including galactic bars at $z \approx 3$ (ref. 80), a disk plus proto-bulge at $z \approx 7$ (ref. 81), and an enigmatic hint that some disk-like galaxies might actually be a population of elongated, or possibly prolate, systems[78,82]. Machine-learning methods, informed by comparisons with simulations, begin to address the scalability of morphological classification (for example, refs. 82–84). Although challenges remain in identifying ongoing mergers from imaging alone, the merger fraction of subpopulations have been quantified out to $z \approx 5$–7 (ref. 85).

Similarly, NIRSpec and the NIRCam grism have opened an unprecedented window into a range of kinematic structures, primarily from gas kinematics. In addition to a diversity of kinematic structures in smaller, Milky Way mass progenitors (for example, refs. 69,86), there are remarkable examples of massive rotating disks in the early Universe[79,87], and a host of non-virial structures in early galaxies driven by stellar and AGN-driven outflows observed in both emission and absorption (for example, refs. 88–90).

### Clustered star formation, proto-globular clusters and single stars

Early galaxies in JWST deep cosmic fields show clumpy stellar structures and overall compact morphologies at scales of several hundred parsecs that dominate the galaxy's UV blue optical light (Fig. 3). With the aid of gravitational lensing, galaxy light has been further broken down into smaller and denser stellar structures (for example, refs. 70,91–94). In some cases, these data reach parsec-scale resolutions, revealing young, massive star clusters in their interiors[95–97]. In general, more than 10% of the total stellar mass observed in these galaxies is in star clusters, which dominate the far-UV light of the host galaxies. The recovered ages show a progression, with the youngest clusters coincident with extreme emission-line equivalent widths and elevated ionizing photon production rate per UV photons ($\xi_{\rm ion}$).

Star clusters detected in early galaxies are consistent with being gravitationally bound, thus, potential proto-globular clusters[95–97]. Their stellar densities are comparable to or higher than globular clusters, enabling runaway stellar and BH mergers in their cores[98]. Radiative and mechanical feedback from these proto-globular clusters is likely to be responsible for the extreme ionization state of these early galaxies, as well as enhanced nitrogen abundances[91,99], which are potentially linked to the chemical pattern of multiple stellar populations found in Milky Way globular clusters[100]. Star clusters within faint $z > 6$ galaxies might be important units for reionization. JWST observations of highly magnified galaxies will be fundamental in characterizing clustered star formation within these early galaxies, through cluster mass functions, cluster formation efficiency and survival rates.

Remarkably, gravitational lensing has also revealed individual stars as distant as Earendel at $z = 6$ (ref. 101). JWST observations have begun revealing their properties, showing that most are hot and luminous O and B stars[102]. Deeper JWST observations could deliver metallicities and outflow wind strengths of individual stars in the early universe[103].

### Chemical enrichment

The metal content of galaxies provides a complementary probe of their integrated past history of star formation, modulated by the inwards and outwards flow of baryons. As such, measurements of galaxy chemical abundances offer essential constraints on the regulation of galaxies over cosmic time. JWST's spectroscopic capabilities have illuminated the build-up of metals within the first billion years, where direct oxygen abundances of roughly 2–30% solar have been measured for a dozen galaxies so far[104–106]. These 'gold standard' direct oxygen abundances are being used to anchor methods based on much brighter emission lines[107,108], which are detected in large samples of galaxies out to $z \approx 10$ (Fig. 4). So far, the highest-redshift measurements of N, C, O, Ne, Ar and S abundances reach as far as $z = 12.5$, only 350 Myr after the Big Bang[109].

Early JWST results demonstrate a continued gradual evolution towards lower total metallicity at fixed stellar mass beyond $z = 4$ (ref. 107), and intriguing evidence for redshift evolution in the baryon cycle at $z > 8$. Specifically, the balance among metallicity, stellar mass and star-formation rate, known as the fundamental metallicity relationship[110], which appears constant from $z \approx 3$ to $z \approx 0$, seems to evolve towards lower metallicity at fixed mass and star-formation rate (for example, ref. 111). This metallicity deficit with respect to the lower-redshift fundamental metallicity relationship appears to increase beyond $z \approx 6$, suggesting that metals are either more efficiently removed by star-formation-driven outflows or more efficiently diluted by inflows of pristine gas at the earliest times. Importantly, JWST has proven to be a powerful 'metal detector' for prominent high-ionization emission lines of C, N and Ne (for example, refs. 7,91,112,113); the abundance patterns of these elements relative to oxygen (for example, C/O and N/O relative to O/H) suggests enrichment by not only core-collapse supernovae[114] but also the winds of massive Wolf–Rayet stars in dense environments such as forming globular clusters[99,115], or even the first generation of supernovae from population III progenitors[109].

So far with JWST, the lowest measured oxygen abundances reach a few per cent of the solar value (for example, refs. 116,117), with evidence reported for one object with abundances below 1% (ref. 118). It remains unclear whether this observed metallicity floor is the result of very rapid chemical enrichment on galactic scales (with associated light-weighted galaxy ages of $\lesssim$5 Myr) or a selection effect. JWST has thus not conclusively identified any first-generation galaxies that are composed entirely of pristine gas and population III, that is, zero metallicity, stars. Nor have we yet seen other signatures of individual first stars, such as those that have been gravitationally lensed, or caught when they explode as the hypothesized pair–instability supernovae.

### Interstellar dust

Characterizing interstellar dust and its effects on starlight in the early Universe is an essential component of tracing the early build-up of galaxies, as well as the evolution of their interstellar contents. JWST has provided an unprecedented view of dust properties in early galaxies. NIRCam photometry and NIRSpec spectroscopy have shown that the rest-UV continuum slopes of star-forming galaxies at $z > 6$ are typically blue, as is characteristic of young, dust-poor systems (for example, refs. 24,25,119,120). These results corroborate previous HST photometric studies of bright galaxies and extend our understanding to a more representative sample, even offering a tantalizing suggestion of dust-free stellar populations at $z > 10$ (ref. 6). JWST has also delivered the first constraints on nebular attenuation using hydrogen recombination lines past $z \approx 2.5$, revealing surprisingly little evolution at fixed stellar mass out to $z \approx 7$ (refs. 121,122). Given the general gas and metal evolution of galaxies, the constancy of attenuation over such a large redshift range is puzzling.

The incredible sensitivity of JWST has enabled the identification of optically faint, dusty sources that had previously eluded detection (for example, refs. 42,123,124). The inclusion of such sources enables a more complete census of early star formation, with roughly twice as much obscured star-formation-rate density inferred at $z \approx 4$–6 (refs. 44,47), compared with pre-JWST estimates.

The properties of dust grains reflect key processes of chemical enrichment, as well as heating and cooling in the interstellar medium. JWST has enabled characterization of the composition and size distribution of the dust grains, with the detection of the 2,175 Å feature at $z = 6.7$, suggesting a rapid formation timescale for carbonaceous grains[125]. The extinction curve seems to flatten at high redshifts, perhaps reflecting a change of the dust grain size distribution, and of the main dust production sources[126].

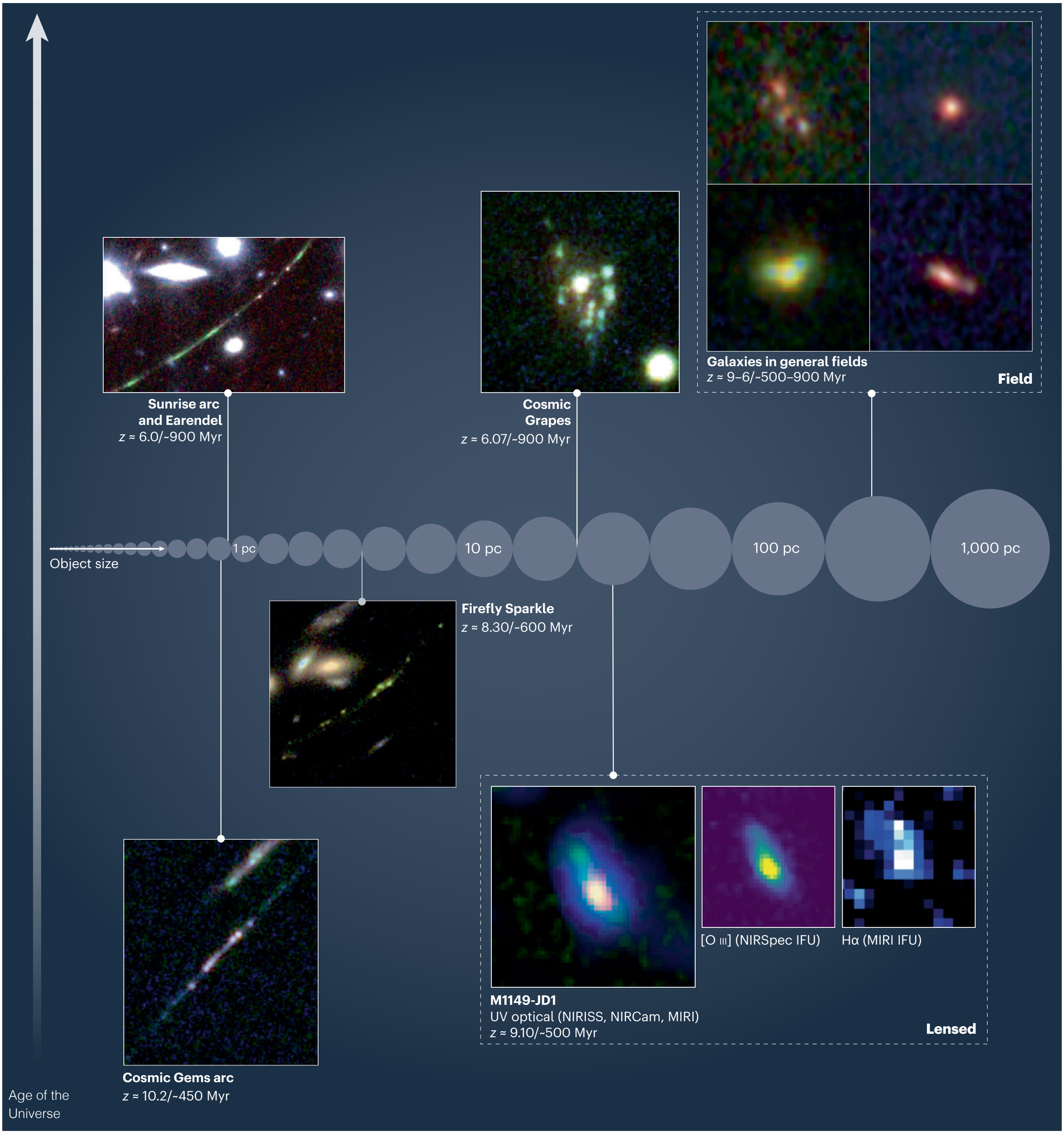


**Fig. 3 | JWST morphologies of galaxies in the first billion years.** Resolved galaxy morphologies at $z > 6$ observed with JWST NIRCam (unless otherwise specified). Galaxies in the field (top) show clumpy and dense structures[75]. Owing to gravitational lensing, the light from these compact galaxies is resolved into several stellar clumps down to scales of tens of parsecs ('Cosmic Grapes'[69]). In some cases, these clumps show strong emission lines as showcased for M1149–JD1 observed with NIRISS and NIRCam[70], MIRI imaging and integral field spectroscopy[180], and NIRSpec (manuscript in preparation by the Galaxy Assembly with NIRSpec Integral Field Spectroscopy (GA-NIFS) collaboration; see https://ga-nifs.github.io) suggesting that intense episodes of star formation are concentrated within them. Near the critical lines, the galaxy light is stretched into long arcs, revealing bright compact bound star clusters, with intrinsic sizes smaller than 10 parsecs ('Cosmic Gems arc'[95], 'Firefly Sparkle'[96] and 'Sunrise arc'[97]) and single stars ('Earendel'[181]). These stellar systems dominate the light of their galaxies, suggesting that star cluster might be a dominant star-formation mode for young galaxies.

## Large-scale environments

Early photometric and grism studies reveal substantially clustered megaparsec-scale distributions of galaxies and AGN beyond $z \gtrsim 5$ (refs. 60,127–129). A typical JWST field contains multiple prominent peaks in the histogram of redshift, spanning overdensities $\delta = 1–100$ on arcminute scales. That high-redshift galaxies would be highly clustered was theorized, following mid-redshift measurements, but it indicates that care must be taken in interpreting the results of

 https://doi.org/10.1038/s41550-025-02624-5

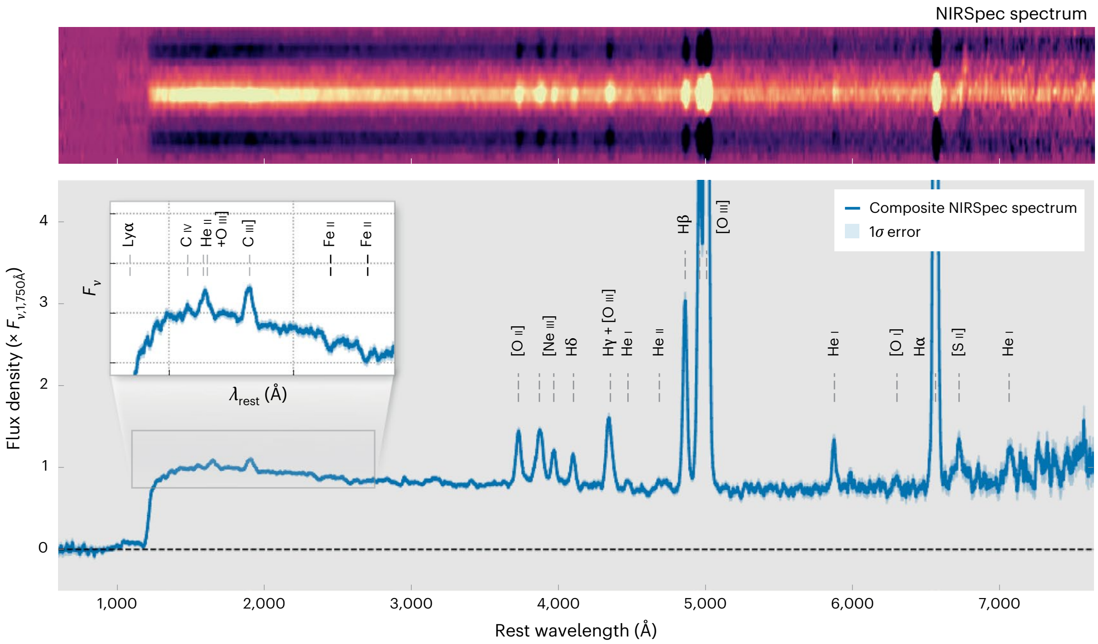


**Fig. 4 | Spectral signatures of early galaxies with JWST.** A composite spectrum using all publicly available $z \geqslant 5$ low-resolution multi-object NIRSpec spectra. The unprecedented sensitivity and wavelength coverage of NIRSpec reveals a plethora of IGM, stellar and ISM features, from Lyman and Balmer breaks to rest-frame UV and optical line emission. The plethora of features allow for characterizations of IGM opacity, stellar ages and masses and gas-phase metallicities, to name a few. *F*, flux density. Figure adapted from ref. 120 under a Creative Commons licence CC BY 4.0.

surveys in single sight-lines and narrow redshift intervals. Substantial field-to-field variations have already been observed (for example, refs. 18,130,131).

Furthermore, at low redshift, it is well known that galaxy properties differ between high- and low-density environments. It is not yet known what high-redshift properties will correlate substantially with environment.

## AGN in early galaxies

Massive BHs are now considered central to galaxy formation and evolution. Many, if not all, galaxies in the local Universe harbour a BH, and empirical relationships between BH mass and the properties of their host galaxies offer compelling evidence of their co-evolution over cosmic time. Detecting and characterizing BHs in the early Universe is crucial for understanding the conditions that drive their formation, their growth, and the initial stages of their interplay and interaction with their host galaxies. Before the advent of JWST, observational studies were limited to detecting the tip of the BH population at high redshift, that is, the most massive accreting BHs. Such observations had confirmed the existence of extremely luminous and rare quasars (bolometric luminosity of $L_{bol} \geqslant 10^{45-46}$ erg s$^{-1}$, ~1 Gpc$^{-3}$) as early as $z \approx 7.6$, powered by BHs of mass $M_{BH} \geqslant 10^8\,M_\odot$. JWST has not only detected the stellar light of these quasars' host galaxies but also uncovered the presence of fainter AGN with $L_{bol} \approx 10^{43-46}$ erg s$^{-1}$ (Fig. 5). The demographics of BHs now encompass objects with masses of ~$10^6$–$10^9\,M_\odot$ at $z \approx 3$–10.

### Demographics and identification

Many candidate AGN have been identified through JWST imaging (broadband, photometric spectral energy distribution (refs. 44,62,132–135 and references therein)). Follow-up spectroscopy has confirmed the presence of AGN at high redshift, with many identifications occurring serendipitously during large spectroscopic surveys. AGN identifications primarily rely on the detection of a broad component of permitted lines, notably Hα, without any counterpart in the forbidden lines (for example, [O III]5,008), ruling out outflows (for example, refs. 136–140 and references therein). The spectral energy distributions of some broad-line or candidate AGN have raised additional puzzles: some are heavily obscured by dust (extinction $A_V \approx 1$–4 (refs. 138,140)), and some less extreme dust-obscured AGN candidates have flatter-than-expected spectral energy distributions at rest frame ⩾1 µm. The latter might indicate that early obscured AGN could lack hot dust emission or that their rest-frame near-infrared is dominated by stars[44,62] (with MIRI imaging).

A large fraction of BH growth could occur in obscured phases; there are now efforts to find these. However, JWST has revealed that some of the standard narrow-line diagnostics used in the local Universe (for example, the so-called Baldwin Phillips & Terlevich (BPT) diagrams) do not work at such high redshift, as AGN seem to overlap with star-forming galaxies, possibly because of low metallicities[14,136,139,141]. Nevertheless, several narrow-line AGN were recently successfully identified from high-ionization UV emission lines (for example, refs. 113,142). Interestingly, most of these AGN could be X-ray weak[143–145], and various reasons are being explored (for example, intrinsic weakness, extreme absorption).

**A large population.** These newly discovered AGN with $L_{bol} \approx 10^{44}$–$10^{46}$ erg s$^{-1}$ appear more numerous than expected from the extrapolation of the luminous quasars' luminosity function, from X-ray selected AGN, or from some cosmological simulations[146]. Specifically, number densities range from $10^{-5}$ mag$^{-1}$ cMpc$^{-3}$ to $10^{-3}$ mag$^{-1}$ cMpc$^{-3}$ in the UV magnitude range $-17 < M_{UV} < -21$ where $M_{UV}$ is the magnitude of the AGN and their hosts[138–140,147].

The fraction of early galaxies hosting an AGN depends strongly on the sensitivity, AGN bolometric luminosity, and whether colour, size or spectroscopic criteria are used, such that the AGN fraction varies from ~1% to ~20%.

**BH masses.** JWST's wavelength range has made it possible to estimate the BH mass of type 1 AGN at high redshift with the same tracers as those used in the local Universe, namely, Balmer broad lines such as Hα and Hβ. This finally enables consistent comparisons across redshift.

https://doi.org/10.1038/s41550-025-02624-5

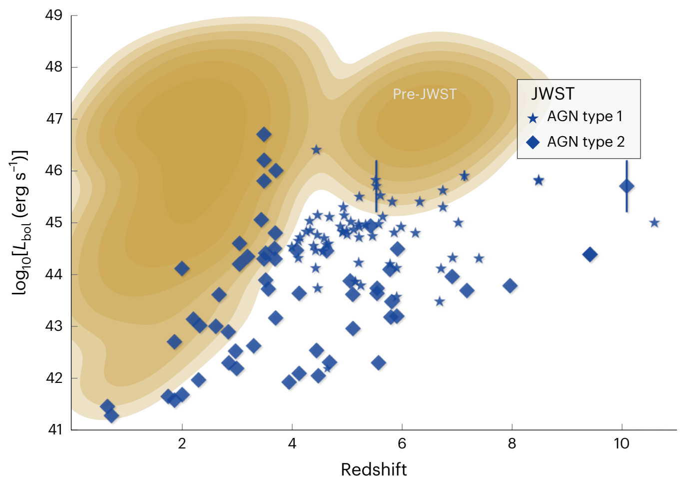


**Fig. 5 | Distribution of bolometric luminosity of known AGN as a function of redshift.** The figure illustrates the discovery space opened by JWST at much lower luminosities and higher redshifts than probed by previous surveys. The brown shaded region shows the range of $L_{bol}$ and redshift spanned by studies before JWST. The blue symbols show a compilation of AGN discovered by JWST, with stars showing type 1 (broad line) AGN and diamonds identifying type 2 (narrow line) AGN. Figure adapted from ref. 142 under a Creative Commons licence CC BY 4.0.

For the small number of high-redshift quasars measured so far, the Balmer-derived masses are consistent with previously derived Mg II masses, within a scatter of 0.5 dex (for example, refs. 148–151).

### Quasar and AGN hosts

JWST data have revealed the stellar light of a few quasar hosts at $z \geqslant 6$ (for example, refs. 152–154), indicating that quasars reside in galaxies with stellar masses of $10^{10-11.5}$ $M_{\odot}$. In addition, the JWST has allowed astronomers to delve into the host properties (stellar mass, velocity dispersion) of the recently discovered AGN at $z \geqslant 4$ with the same tracers as used in the local and low-redshift Universe, and has already raised intriguing questions. Such AGN seem to be embedded in galaxies with stellar masses of $10^{8-10.5}$ $M_{\odot}$. Both these newly discovered AGN and high-redshift quasars have high BH-to-stellar-mass ratios compared with those of the local Universe[112,141,147,155,156]. This finding may support scenarios involving heavy seeds (direct-collapse BHs) and/or bursts of super-Eddington accretion during the early phases of BH growth. However, selection effects and uncertainties in both BH and stellar masses can play a role.

### Quasar large-scale environment

The question of which environments can drive the rapid assembly of extremely massive, high-redshift quasars in less than 1 Gyr has remained a long-standing challenge until recently. JWST data have not only spectroscopically confirmed that quasars have close companions[149,157] but also demonstrated that some quasars are embedded in overdense environments, with an enhanced number of [O III] emitters on megaparsec scales[129], while others live in fields consistent with the average density of the Universe[130].

JWST will be key to disentangling whether this is due to a broad range of quasar dark matter haloes and/or the consequence of quasar feedback into their surroundings.

### Implications for BH seeding and growth

Before JWST, the existence of quasars at $z \geqslant 6$ suggested that their progenitors, referred to as BH seeds, must have formed with masses ranging from a few hundred solar masses ('light seeds' formed from the remnants of population III stars) to about a million solar masses ('heavy seeds') in the very early Universe. While JWST has not ruled out any of the existing theoretical models, the confirmation of overmassive BHs (with high BH-to-stellar-mass ratios) could hint towards the existence of heavy seed channel(s). Those can form, for example, from the collapse of high peak density fluctuations ('primordial BHs'), the collapse of supermassive stars formed in atomic cooling haloes ('direct collapse' seeds with ~$10^{3-5}$ $M_{\odot}$) or through hierarchical mergers of massive stars or BHs in compact stellar clusters (seeds with ~$10^{2-3}$ $M_{\odot}$).

Additional solutions to the abundance of AGN and overmassive BHs include sustained super-Eddington accretion and BH mergers. Super-Eddington phases can account for a large fraction of BH growth under reduced BH feedback as shown in models[158–160] and supported by recent observational findings[112,156]. The contribution of BH mergers in their mass budget remains a long-standing question, tied to their mass, dynamics and environment. Remarkably, JWST has already revealed the existence of dual AGN at high redshift with separations of a few/several kiloparsec[161,162]; a population surprisingly larger (by about an order of magnitude) than what is predicted by cosmological simulations. In addition, there are growing indications of dual AGN on even smaller scales of a few 100 pc, which are probably in the process of merging[137,139].

## Reionization

The collective energy of the first stars, galaxies and accreting BHs—including those too faint for even JWST to detect directly—transform the universe around them by heating and ionizing hydrogen (and later helium) gas in the intergalactic medium. This 'reionization' process sets the stage for all subsequent galaxy formation, as it impacts the ability of future dwarf galaxies to cool gas and form stars. We know that hydrogen reionization happened, but exactly when and how it happened has been a major missing piece in our understanding of the first billion years.

Assuming that reionization is driven by stars in early galaxies, the energy injection is commonly simply parameterized by the product of three terms. (1) The UV luminosity density of sources, $\rho_{UV}(z)$, which describes the total abundance of high-redshift ionizing sources, as discussed above. (2) The production rate of hydrogen ionizing photons per UV photons, $\xi_{ion}$, determined by the stellar populations. (3) The fraction of ionizing photons that escape the dense interstellar medium (ISM) of galaxies into the intergalactic medium (IGM), $f_{esc}$. The rate of ionization is determined by the evolution of these quantities with redshift and galaxy properties, and the rate of hydrogen recombination in the IGM.

Before JWST, we knew that reionization ended approximately 1 billion years after the Big Bang ($z \approx 5$–$6$), but not when it started. Owing to the limited observations of the UV luminosity function for galaxies and AGNs, and local Universe indications that the escape fraction of ionizing photons from galaxies was modest (<5%), the ionizing photon budget was tight. It was commonly assumed that reionization was accomplished by dwarf ($M_{UV} \approx -13$) galaxies, by extrapolating a UV luminosity function steep at the faint end (slope ~−2), and assuming escape fractions 10–20%. Owing to the low observed number densities of UV-bright $z > 6$ AGN, they were commonly assumed to not play a major role in hydrogen reionization.

### Sources of reionization

With the JWST, we have made significant progress in understanding the reionization process. The JWST has shown that the ionizing photon budget is not necessarily tight and that high average values (>20%) of the escape fraction are not necessary. As discussed above, we have now been able to measure the faint end of the UV luminosity function at least up to $z \approx 7$–$8$, and obtained information on the UV luminosity density of $M_{UV} < -17$ sources within the first billion years. We have also obtained hints on the variability of star formation of these sources. We have found spectroscopically confirmed galaxies up to $z = 14.3$, implying that reionization may have started just a few hundred million years after the Big Bang.

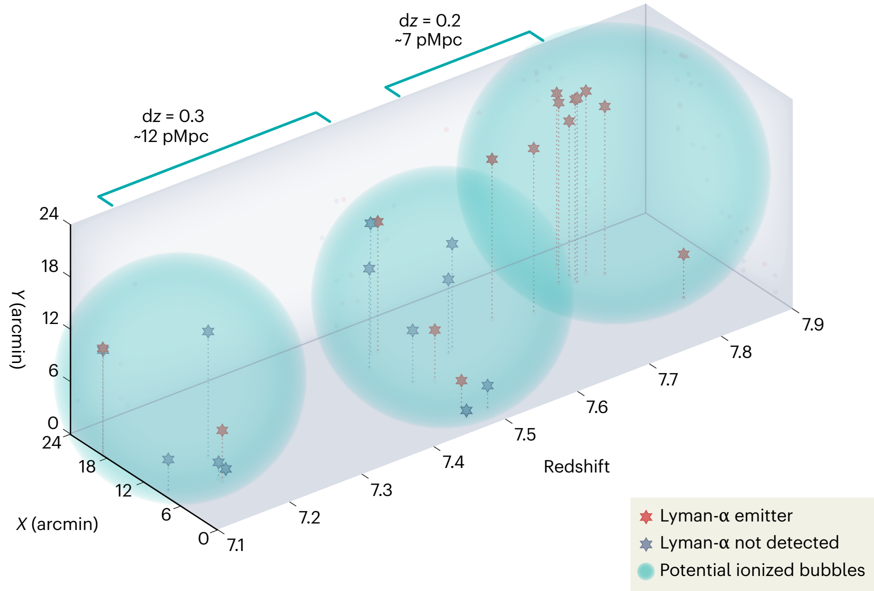


**Fig. 6 | Potential ionized bubbles in the reionization era.** Spectroscopically confirmed galaxies in the Cosmic Evolution Early Release Science Survey, Extended Groth Strip field at $z = 7.1$–$7.8$. The presence of numerous Lyman-α emitting galaxies (red stars), including several with high equivalent widths (>200 Å) and Lyman-α escape fractions (≳50%), in this field provides strong evidence for candidate ionized bubbles along the line of sight (shaded cyan regions—for illustration purposes only). These early observations, primarily of $M_{UV} < -19$ HST-selected sources, highlight the potential of JWST to create tomographic maps of ionized regions to learn about the reionization process on local scales. Figure adapted from ref. 172 under a Creative Commons licence CC BY 4.0.

JWST has spectroscopically measured the ionizing photon production of galaxies down to $M_{UV} = -15.5$ (ref. 116). Direct measurements of $\xi_{ion}$ from photometry and spectra of Balmer lines up to $z \approx 6$–$9$ (refs. 60,120,163,164) find a range of values, $\log\xi_{ion} \approx 26$–$26$ erg$^{-1}$ Hz, likely implying that galaxies have a range of star-formation histories. Mean $\xi_{ion}$ values are about three times higher than pre-JWST assumptions, reducing the need for high escape fractions. These values reflect larger populations of hot, massive stars and may be driven by more recently rising star-formation histories, lower metallicity or possibly more top-heavy IMFs (for example, ref. 66).

JWST's discovery and characterization of faint AGN at $z > 5$ (see above) has opened new discussions on the AGN contribution to reionization. However, as the majority of these high-redshift AGN are probably UV-obscured or intrinsically faint, BH accretion likely contributes no more than 25% to ionizing budget[165].

There is still significant debate about the primary sources of reionization, in particular the contribution of faint galaxies ($M_{UV} < -17$). This is driven by uncertainties in the galaxy properties including the 'burstiness' of the star-formation history, the IMF and $f_{esc}$. The foreground neutral IGM makes direct measurement of $f_{esc}$ impossible within the epoch of reionization. Therefore, JWST observations are being combined with those from ground-based telescopes and HST to identify galaxy properties that correlate with $f_{esc}$ in the $z < 3$ Universe, where direct observations of ionizing photons are possible. These correlations imply modest average $f_{esc}$ (≲10%) values in samples of tens of $z > 6$ sources where comparisons with $z < 3$ galaxies are possible (for example, refs. 166,167).

In summary, recent JWST observations have found that early galaxies were more numerous and more efficient producers of ionizing photons than previously assumed. While there is still significant uncertainty about their star-formation histories and escape fractions, we have moved from a situation where we thought that there were not enough ionizing photons to complete reionization to one where we might have an excess. Significant progress should be expected with future JWST observations by surveying the faint ($M_{UV} > -17$) galaxy population with deeper imaging and spectroscopy to understand their contribution to reionization.

## Morphology and growth of ionized regions

JWST is also enabling us to observe the reionization process directly. Reionization is predicted to be 'patchy', with ionized bubbles growing around overdensities of galaxies (Fig. 6). The ionization state of the IGM can be traced by transmission of Lyman-series photons—either through the Lyman-α and -β forest, probing the very end stages of reionization at $z \approx 6$, or Lyman-α emission from galaxies at all stages of reionization. The JWST has shown that the $z \approx 6$ Lyman-α and -β forest transmission measured in quasar spectra is correlated with distance from galaxies, suggesting that galaxies (and their overdensities) dominated the ionizing emissivity at $z \approx 6$ (ref. 128). A downturn in the average Lyman-α emission from galaxies at $z \gtrsim 6$ has been confirmed[168,169], implying that we are observing a predominantly neutral universe at higher redshifts. JWST spectroscopy enables us to infer the ionization state of the IGM at $z > 10$ (ref. 170), hence providing an independent constraint on the total star-formation rate density at early times, probing sources below the detection limits of even JWST.

The JWST also finds strong evidence for ionized regions, giving the first opportunity to understand how reionization is occurring on local scales. Early results have shown large field-to-field variations in Lyman-α emission visibility, even in overdensities[171–173], and also highlighted the importance of understanding Lyman-α absorption by dense residual neutral gas within and around galaxies[93,172,174]. The sizes of ionized regions are predicted to be determined by the clustering strength, luminosity and star-formation histories of the dominant reionizing sources (for example, ref. 175) and can be probed directly via the spatial variations in Lyman-α transmission.

JWST has enabled the first measurements of Lyman-α escape fractions (from Balmer lines), robust fluxes and velocity offsets from systemic in $z > 7$ galaxies. The discovery of sources with high Lyman-α rest-frame equivalent width and Lyman-α escape fraction, and low-velocity offsets, in overdense regions implies these galaxies reside in ionized regions ≳1 pMpc (refs. 172,176,177). By spectroscopically confirming galaxies in these regions, we are starting to build three-dimensional maps[172,178] (Fig. 6), which probe the contribution to reionization from faint sources below the detection limits of JWST[59].

Future systematic spectroscopic studies of Lyman-α visibility as a function of environment and galaxy properties will help us understand how ionized regions grew. This will enable us to constrain ionizing photon escape fractions and star formation in sources beyond the detection limits of the JWST.

## Conclusion

JWST's sharp imaging, broad wavelength coverage, exquisite spectroscopy and two-orders-of-magnitude improvement in sensitivity have unlocked the study of how galaxies evolved in the first billion years. The high-redshift Universe has emerged in stunning definition and the initial discoveries of JWST are rewriting astronomy textbooks.

The JWST has revealed that galaxies and BHs assembled, formed significant stellar mass and dust, and synthesized the elements of the periodic table much earlier than was expected. The remarkable abundance of luminous and potentially massive galaxies at such early times hold the promise of upending theories of primordial galaxy formation. The discovery of very dense and massive star clusters urge us to decipher the role that these tiny stellar systems play in the evolution of early galaxies. The large numbers and apparent high masses of accreting supermassive BHs found by the JWST have renewed interest in channels that generate intermediate-mass seeds. The JWST has directly measured the abundance of chemical elements in these early galaxies, finding low ($\gtrsim$2%) but non-zero oxygen abundance, which indicates either that the Universe rapidly self-enriched or that the JWST has not yet reached the epoch of the very first galaxies. Whereas before the JWST we knew that the Universe must have reionized, but did not know which sources were responsible, The JWST has now found thousands of galaxies in the epoch of reionization, and associated individual ionized bubbles with star-forming galaxies, beginning to map out the topology of reionization.

We are gathering many pieces in the puzzle that describes the chronology of the first billion years of the Universe; however, the emerging picture is still scattered. In the coming years, as many more discoveries are made, we will be able to connect these subfields, and comprehensively describe the first billion years of cosmic history.

## References


1. Rigby, J. et al. The science performance of JWST as characterized in commissioning. *Publ. Astron. Soc. Pac.* **135**, 048001 (2023).
2. Planck Collaborationet al. Planck 2018 results. VI. Cosmological parameters. *Astron. Astrophys.* **641**, A6 (2020).
3. Atek, H. et al. Revealing galaxy candidates out to $z \sim 16$ with JWST observations of the lensing cluster SMACS0723. *Mon. Not. R. Astron. Soc.* **519**, 1201–1220 (2023).
4. Harikane, Y. et al. Pure spectroscopic constraints on UV luminosity functions and cosmic star formation history from 25 galaxies at $z_{spec}$ = 8.61–13.20 confirmed with JWST/NIRSpec. *Astrophys. J.* **960**, 56 (2024).
5. Hsiao, T. Y.-Y. et al. JWST reveals a possible $z \sim 11$ galaxy merger in triply lensed MACS0647–JD. *Astrophys. J. Lett.* **949**, L34 (2023).
6. Curtis-Lake, E. et al. Spectroscopic confirmation of four metal-poor galaxies at $z$ = 10.3–13.2. *Nat. Astron.* **7**, 622–632 (2023).
7. Bunker, A. J. et al. JADES NIRSpec initial data release for the Hubble Ultra Deep Field: redshifts and line fluxes of distant galaxies from the deepest JWST Cycle 1 NIRSpec multi-object spectroscopy. *Astron. Astrophys.* **690**, A288 (2024).
8. Arrabal Haro, P. et al. Spectroscopic confirmation of CEERS NIRCam-selected galaxies at $z$ = 8–10. *Astrophys. J. Lett.* **951**, L22 (2023).
9. Finkelstein, S. L. et al. CEERS key paper. I. An early look into the first 500 Myr of galaxy formation with JWST. *Astrophys. J. Lett.* **946**, L13 (2023).
10. Castellano, M. et al. JWST NIRSpec spectroscopy of the remarkable bright galaxy GHZ2/GLASS-z12 at redshift 12.34. *Astrophys. J.* **972**, 143 (2024).
11. Carniani, S. et al. Spectroscopic confirmation of two luminous galaxies at a redshift of 14. *Nature* **633**, 318–322 (2024).
12. Donnan, C. T. et al. JWST PRIMER: a new multifield determination of the evolving galaxy UV luminosity function at redshifts $z \simeq$ 9–15. *Mon. Not. R. Astron. Soc.* **533**, 3222–3237 (2024).
13. Bouwens, R. J. et al. Evolution of the UV LF from $z \sim 15$ to $z \sim 8$ using new JWST NIRCam medium-band observations over the HUDF/XDF. *Mon. Not. R. Astron. Soc.* **523**, 1036–1055 (2023).
14. Harikane, Y. et al. A comprehensive study of galaxies at $z \sim$ 9–16 found in the early JWST data: ultraviolet luminosity functions and cosmic star formation history at the pre-reionization epoch. *Astrophys. J. Suppl. Ser.* **265**, 5 (2023).
15. Pérez-González, P. G. et al. Life beyond 30: probing the $-20 < M_{UV} < -17$ luminosity function at $8 < z < 13$ with the NIRCam parallel field of the MIRI Deep Survey. *Astrophys. J. Lett.* **951**, L1 (2023).
16. McLeod, D. J. et al. The galaxy UV luminosity function at $z$ = 11 from a suite of public JWST ERS, ERO, and Cycle-1 programs. *Mon. Not. R. Astron. Soc.* **527**, 5004–5022 (2024).
17. Robertson, B. et al. Earliest galaxies in the JADES Origins Field: luminosity function and cosmic star formation rate density 300 Myr after the Big Bang. *Astrophys. J.* **970**, 31 (2024).
18. Willott, C. J. et al. A steep decline in the galaxy space density beyond redshift 9 in the CANUCS UV luminosity function. *Astrophys. J.* **966**, 74 (2024).
19. Naidu, R. P. et al. Two remarkably luminous galaxy candidates at $z \approx$ 10–12 revealed by JWST. *Astrophys. J. Lett.* **940**, L14 (2022).
20. Finkelstein, S. L. et al. The complete CEERS early universe galaxy sample: a surprisingly slow evolution of the space density of bright galaxies at $z \sim$ 8.5–14.5. *Astrophys. J. Lett.* **969**, L2 (2024).
21. Leung, G. C. K. et al. NGDEEP epoch 1: the faint end of the luminosity function at $z \sim$ 9–12 from ultradeep JWST imaging. *Astrophys. J. Lett.* **954**, L46 (2023).
22. Chemerynska, I. et al. JWST UNCOVER: the overabundance of ultraviolet-luminous galaxies at $z > 9$. *Mon. Not. R. Astron. Soc.* **531**, 2615–2625 (2024).
23. Casey, C. M. et al. COSMOS-Web: intrinsically luminous $z \gtrsim 10$ galaxy candidates test early stellar mass assembly. *Astrophys. J.* **965**, 98 (2024).
24. Topping, M. W. et al. The UV continuum slopes of early star-forming galaxies in JADES. *Mon. Not. R. Astron. Soc.* **529**, 4087–4103 (2024).
25. Cullen, F. et al. The ultraviolet continuum slopes of high-redshift galaxies: evidence for the emergence of dust-free stellar populations at $z > 10$. *Mon. Not. R. Astron. Soc.* **531**, 997–1020 (2024).
26. Wilkins, S. M. et al. First Light and Reionization Epoch Simulations (FLARES) V: the redshift frontier. *Mon. Not. R. Astron. Soc.* **519**, 3118–3128 (2023).
27. Mauerhofer, V. & Dayal, P. The dust enrichment of early galaxies in the JWST and ALMA era. *Mon. Not. R. Astron. Soc.* **526**, 2196–2209 (2023).
28. Ferrara, A., Pallottini, A. & Dayal, P. On the stunning abundance of super-early, luminous galaxies revealed by JWST. *Mon. Not. R. Astron. Soc.* **522**, 3986–3991 (2023).
29. Ferrara, A. Super-early JWST galaxies, outflows, and Lyα visibility in the epoch of reionization. *Astron. Astrophys.* **684**, A207 (2024).
30. Mason, C. A., Trenti, M. & Treu, T. The brightest galaxies at cosmic dawn. *Mon. Not. R. Astron. Soc.* **521**, 497–503 (2023).
31. Mirocha, J. & Furlanetto, S. R. Balancing the efficiency and stochasticity of star formation with dust extinction in $z \gtrsim 10$ galaxies observed by JWST. *Mon. Not. R. Astron. Soc.* **519**, 843–853 (2023).
32. Pallottini, A. & Ferrara, A. Stochastic star formation in early galaxies: Implications for the James Webb Space Telescope. *Astron. Astrophys.* **677**, L4 (2023).

33. Dekel, A., Sarkar, K. C., Birnboim, Y., Mandelker, N. & Li, Z. Efficient formation of massive galaxies at cosmic dawn by feedback-free starbursts. *Mon. Not. R. Astron. Soc.* **523**, 3201–3218 (2023).
34. Li, Z. et al. Feedback-free starbursts at cosmic dawn: observable predictions for JWST. *Astron. Astrophys.* **690**, A108 (2024).
35. Inayoshi, K., Harikane, Y., Inoue, A. K., Li, W. & Ho, L. C. A lower bound of star formation activity in ultra-high-redshift galaxies detected with JWST: implications for stellar populations and radiation sources. *Astrophys. J. Lett.* **938**, L10 (2022).
36. Rasmussen Cueto, E. R. et al. ASTRAEUS. IX. Impact of an evolving stellar initial mass function on early galaxies and reionisation. *Astron. Astrophys.* **686**, A138 (2024).
37. Liu, B. & Bromm, V. Accelerating early massive galaxy formation with primordial black holes. *Astrophys. J. Lett.* **937**, L30 (2022).
38. Moffat, J. W. Galaxy formation in the early Universe. Preprint at https://arxiv.org/abs/2412.03534 (2024).
39. Menci, N., Adil, S. A., Mukhopadhyay, U., Sen, A. A. & Vagnozzi, S. Negative cosmological constant in the dark energy sector: tests from JWST photometric and spectroscopic observations of high-redshift galaxies. *J. Cosmol. Astropart. Phys.* **2024**, 072 (2024).
40. Harvey, T. et al. EPOCHS IV: SED modelling assumptions and their impact on the stellar mass function at $6.5 \le z \le 13.5$ using PEARLS and public JWST observations. *Astrophys. J.* **978**, 89 (2025).
41. Weibel, A., Oesch, P. & Barrufet, L. et al. Galaxy build-up in the first 1.5 Gyr of cosmic history: insights from the stellar mass function at $z \sim 4$–9 from JWST NIRCam observations. *Mon. Not. R. Astron. Soc.* **533**, 1808–1838 (2024).
42. Barrufet, L. et al. Unveiling the nature of infrared bright, optically dark galaxies with early JWST data. *Mon. Not. R. Astron. Soc.* **522**, 449–456 (2023).
43. Gottumukkala, R. et al. Unveiling the hidden universe with JWST: the contribution of dust-obscured galaxies to the stellar mass function at $z \sim 3$–8. *Mon. Not. R. Astron. Soc.* **530**, 966–983 (2024).
44. Williams, C. C. et al. The galaxies missed by Hubble and ALMA: the contribution of extremely red galaxies to the cosmic census at $3 < z < 8$. *Astrophys. J.* **968**, 34 (2024).
45. Wang, T. et al. Massive galaxies across cosmic time revealed by JWST/MIRI (MACROSS): the true number density of massive galaxies in the early Universe. Preprint at https://arxiv.org/abs/2403.02399 (2024).
46. Labbé, I. et al. A population of red candidate massive galaxies 600 Myr after the Big Bang. *Nature* **616**, 266–269 (2023).
47. Xiao, M. et al. Accelerated formation of ultra-massive galaxies in the first billion years. *Nature* **635**, 311–315 (2024).
48. Boylan-Kolchin, M. Stress testing $\Lambda$CDM with high-redshift galaxy candidates. *Nat. Astron.* **7**, 731–735 (2023).
49. Desprez, G. et al. $\Lambda$CDM not dead yet: massive high-$z$ Balmer break galaxies are less common than previously reported. *Mon. Not. R. Astron. Soc.* **530**, 2935–2952 (2024).
50. Kocevski, D. D. et al. CEERS key paper. II. A first look at the resolved host properties of AGN at $3 < z < 5$ with JWST. *Astrophys. J. Lett.* **946**, L14 (2023).
51. Carnall, A. C. et al. A massive quiescent galaxy at redshift 4.658. *Nature* **619**, 716–719 (2023).
52. Glazebrook, K. et al. A massive galaxy that formed its stars at $z \sim 11$. *Nature* **628**, 277–281 (2024).
53. Nanayakkara, T. et al. A population of faint, old, and massive quiescent galaxies at $3 < z < 4$ revealed by JWST NIRSpec spectroscopy. *Sci. Rep.* **14**, 3724 (2024).
54. Setton, D. J. et al. UNCOVER NIRSpec/PRISM spectroscopy unveils evidence of early core formation in a massive, centrally dusty quiescent galaxy at $z_{\rm spec} = 3.97$. *Astrophys. J.* **974**, 145 (2024).
55. Carnall, A. C. et al. A surprising abundance of massive quiescent galaxies at $3 < z < 5$ in the first data from JWST CEERS. *Mon. Not. R. Astron. Soc.* **520**, 3974–3985 (2023).
56. Valentino, F. et al. An atlas of color-selected quiescent galaxies at $z > 3$ in public JWST fields. *Astrophys. J.* **947**, 20 (2023).
57. Sun, G., Faucher-Giguère, C.-A., Hayward, C. C. & Shen, X. Seen and unseen: bursty star formation and its implications for observations of high-redshift galaxies with JWST. *Mon. Not. R. Astron. Soc.* **526**, 2665–2672 (2023).
58. Whitler, L. et al. On the ages of bright galaxies 500 Myr after the Big Bang: insights into star formation activity at $z \gtrsim 15$ with JWST. *Mon. Not. R. Astron. Soc.* **519**, 157–171 (2023).
59. Whitler, L. et al. Insight from JWST/NIRCam into galaxy overdensities around bright Lyman-alpha emitters during reionization: implications for ionized bubbles at $z \sim 9$. *Mon. Not. R. Astron. Soc.* **529**, 855–872 (2024).
60. Endsley, R. et al. The star-forming and ionizing properties of dwarf $z \sim 6$–9 galaxies in JADES: insights on bursty star formation and ionized bubble growth. *Mon. Not. R. Astron. Soc.* **533**, 1111–1142 (2024).
61. Carnall, A. C. et al. A first look at the SMACS0723 JWST ERO: spectroscopic redshifts, stellar masses, and star-formation histories. *Mon. Not. R. Astron. Soc.* **518**, L45–L50 (2023).
62. Pérez-González, P. G. et al. What is the nature of Little Red Dots and what is not, MIRI SMILES edition. *Astrophys. J.* **968**, 4 (2024).
63. Looser, T. J. et al. A recently quenched galaxy 700 million years after the Big Bang. *Nature* **629**, 53–57 (2024).
64. Strait, V. et al. An extremely compact, low-mass galaxy on its way to quiescence at $z = 5.2$. *Astrophys. J. Lett.* **949**, L23 (2023).
65. Topping, M. W. et al. Searching for extremely blue UV continuum slopes at $z = 7$–11 in JWST/NIRCam imaging: implications for stellar metallicity and ionizing photon escape in early galaxies. *Astrophys. J.* **941**, 153 (2022).
66. Endsley, R. et al. A JWST/NIRCam study of key contributors to reionization: the star-forming and ionizing properties of UV-faint $z \sim 7$–8 galaxies. *Mon. Not. R. Astron. Soc.* **524**, 2312–2330 (2023).
67. Looser, T. J. et al. JADES: differing assembly histories of galaxies: observational evidence for bursty star-formation histories and (mini-)quenching in the first billion years of the Universe. *Astron. Astrophys.* **697**, A88 (2024).
68. Giménez-Arteaga, C. et al. Spatially resolved properties of galaxies at $5 < z < 9$ in the SMACS 0723 JWST ERO field. *Astrophys. J.* **948**, 126 (2023).
69. Fujimoto, S. et al. Primordial rotating disk composed of at least 15 dense star-forming clumps at cosmic dawn. *Nat. Astron.* (in the press).
70. Bradač, M. et al. Star formation at the epoch of reionization with CANUCS: the ages of stellar populations in MACS1149–JD1. *Astrophys. J. Lett.* **961**, L21 (2024).
71. Cutler, S. E. et al. Two distinct classes of quiescent galaxies at cosmic noon revealed by JWST PRIMER and UNCOVER. *Astrophys. J. Lett.* **967**, L23 (2024).
72. Yang, L. et al. Early results from GLASS-JWST. V: the first rest-frame optical size–luminosity relation of galaxies at $z > 7$. *Astrophys. J. Lett.* **938**, L17 (2022).
73. Morishita, T. & Stiavelli, M. Physical characterization of early galaxies in the Webb's First Deep Field SMACS J0723.3–7323. *Astrophys. J. Lett.* **946**, L35 (2023).
74. Ito, K. et al. Size–stellar mass relation and morphology of quiescent galaxies at $z \ge 3$ in public JWST fields. *Astrophys. J.* **964**, 192 (2024).
75. Kartaltepe, J. S. et al. CEERS key paper. III. The diversity of galaxy structure and morphology at $z = 3$–9 with JWST. *Astrophys. J. Lett.* **946**, L15 (2023).
76. Robertson, B. E. et al. Morpheus reveals distant disk galaxy morphologies with JWST: the first AI/ML analysis of JWST images. *Astrophys. J. Lett.* **942**, L42 (2023).

77. Treu, T. et al. Early results from GLASS-JWST. XII. The morphology of galaxies at the epoch of reionization. *Astrophys. J. Lett.* **942**, L28 (2023).
78. Pandya, V. et al. Galaxies going bananas: inferring the 3D geometry of high-redshift galaxies with JWST-CEERS. *Astrophys. J.* **963**, 54 (2024).
79. Nelson, E. J. et al. JWST reveals a population of ultrared, flattened galaxies at $2 \lesssim z \lesssim 6$ previously missed by HST. *Astrophys. J. Lett.* **948**, L18 (2023).
80. Costantin, L. et al. A Milky Way-like barred spiral galaxy at a redshift of 3. *Nature* **623**, 499–501 (2023).
81. Baker, W. M. et al. A core in a star-forming disc as evidence of inside-out growth in the early Universe. *Nat. Astron.* **9**, 141–154 (2025).
82. Vega-Ferrero, J. et al. On the nature of disks at high redshift seen by JWST/CEERS with contrastive learning and cosmological simulations. *Astrophys. J.* **961**, 51 (2024).
83. Huertas-Company, M. et al. Galaxy morphology from $z$~ 6 through the eyes of JWST. *Astron. Astrophys.* **685**, A48 (2024).
84. Tohill, C. et al. A robust study of high-redshift galaxies: unsupervised machine learning for characterizing morphology with JWST up to $z$ ~ 8. *Astrophys. J.* **962**, 164 (2024).
85. Asada, Y. et al. Bursty star formation and galaxy-galaxy interactions in low-mass galaxies 1 Gyr after the Big Bang. *Mon. Not. R. Astron. Soc.* **527**, 11372–11392 (2024).
86. de Graaff, A. et al. Ionised gas kinematics and dynamical masses of $z \gtrsim 6$ galaxies from JADES/NIRSpec high-resolution spectroscopy. *Astron. Astrophys.* **684**, A87 (2024).
87. Arribas, S. et al. GA-NIFS: the core of an extremely massive proto-cluster at the epoch of reionization probed with JWST/NIRSpec. *Astron. Astrophys.* **688**, A146 (2024).
88. Carniani, S. et al. JADES: the incidence rate and properties of galactic outflows in low-mass galaxies across $3<z<9$. *Astron. Astrophys.* **685**, A99 (2024).
89. D'Eugenio, F. et al. A fast-rotator post-starburst galaxy quenched by supermassive black-hole feedback at $z$=3. *Nat. Astron.* **9**, 1443–1456 (2024).
90. Belli, S. et al. Star formation shut down by multiphase gas outflow in a galaxy at a redshift of 2.45. *Nature* **630**, 54–58 (2024).
91. Topping, M. W. et al. Metal-poor star formation at $z > 6$ with JWST: new insight into hard radiation fields and nitrogen enrichment on 20 pc scales. *Mon. Not. R. Astron. Soc.* **529**, 3301–3322 (2024).
92. Williams, H. et al. A magnified compact galaxy at redshift 9.51 with strong nebular emission lines. *Science* **380**, 416–420 (2023).
93. Hsiao, T. Y.-Y. et al. JWST NIRSpec spectroscopy of the triply-lensed $z$=10.17 galaxy MACS0647–JD. *Astrophys. J.* **973**, 8 (2024).
94. Claeyssens, A. et al. Star formation at the smallest scales: a JWST study of the clump populations in SMACS0723. *Mon. Not. R. Astron. Soc.* **520**, 2180–2203 (2023).
95. Vanzella, E. et al. JWST/NIRCam probes young star clusters in the reionization era Sunrise arc. *Astrophys. J.* **945**, 53 (2023).
96. Adamo, A. et al. Bound star clusters observed in a lensed galaxy 460 Myr after the Big Bang. *Nature* **632**, 513–516 (2024).
97. Mowla, L. et al. Formation of a low-mass galaxy from star clusters in a 600-million-year-old Universe. *Nature* **636**, 332–336 (2024).
98. Antonini, F., Gieles, M., Dosopoulou, F. & Chattopadhyay, D. Coalescing black hole binaries from globular clusters: mass distributions and comparison to gravitational wave data from GWTC-3. *Mon. Not. R. Astron. Soc.* **522**, 466–476 (2023).
99. Cameron, A. J., Katz, H., Rey, M. P. & Saxena, A. Nitrogen enhancements 440 Myr after the big bang: supersolar N/O, a tidal disruption event, or a dense stellar cluster in GN-z11? *Mon. Not. R. Astron. Soc.* **523**, 3516–3525 (2023).
100. Gratton, R. et al. What is a globular cluster? An observational perspective. *Astron. Astrophys. Rev.* **27**, 8 (2019).
101. Welch, B. et al. TEMPLATES: direct abundance constraints for two lensed Lyman-break galaxies. *Astrophys. J.* **975**, 196 (2024).
102. Meena, A. K. et al. Two lensed star candidates at $z$ = 4.8 behind the galaxy cluster MACS J0647.7+7015. *Astrophys. J. Lett.* **944**, L6 (2023).
103. Lundqvist, E., Zackrisson, E., Hawcroft, C., Amarsi, A. M. & Welch, B. Spectroscopic characterisation of gravitationally lensed stars at high redshifts. *Astron. Astrophys.* **690**, A291 (2024).
104. Schaerer, D. et al. First look with JWST spectroscopy: resemblance among $z$ ~ 8 galaxies and local analogs. *Astron. Astrophys.* **665**, L4 (2022).
105. Laseter, I. H. et al. JADES: detecting [OIII]λ4363 emitters and testing strong line calibrations in the high-$z$ Universe with ultra-deep JWST/NIRSpec spectroscopy up to $z$ ~ 9.5. *Astron. Astrophys.* **681**, A70 (2024).
106. Sanders, R. L., Shapley, A. E., Topping, M. W., Reddy, N. A. & Brammer, G. B. Direct $T_e$-based metallicities of $z$ = 2–9 galaxies with JWST/NIRSpec: empirical metallicity calibrations applicable from reionization to cosmic noon. *Astrophys. J.* **962**, 24 (2024).
107. Nakajima, K. et al. JWST census for the mass–metallicity star formation relations at $z$ = 4–10 with self-consistent flux calibration and proper metallicity calibrators. *Astrophys. J. Suppl. Ser.* **269**, 33 (2023).
108. Sanders, R. L. et al. A preview of JWST metallicity studies at cosmic noon: the first detection of auroral [O II] emission at high redshift. *Astrophys. J.* **943**, 75 (2023).
109. D'Eugenio, F. et al. JADES: carbon enrichment 350 Myr after the Big Bang. *Astron. Astrophys.* **689**, A152 (2024).
110. Mannucci, F., Cresci, G., Maiolino, R., Marconi, A. & Gnerucci, A. A fundamental relation between mass, star formation rate and metallicity in local and high-redshift galaxies. *Mon. Not. R. Astron. Soc.* **408**, 2115–2127 (2010).
111. Curti, M. et al. JADES: insights into the low-mass end of the mass–metallicity–star-formation rate relation at $3 < z < 10$ from deep JWST/NIRSpec spectroscopy. *Astron. Astrophys.* **684**, A75 (2024).
112. Maiolino, R. et al. A small and vigorous black hole in the early Universe. *Nature* **627**, 59–63 (2024).
113. Chisholm, J. et al. [Ne V] emission from a faint epoch of reionization-era galaxy: evidence for a narrow-line intermediate-mass black hole. *Mon. Not. R. Astron. Soc.* **534**, 2633–2656 (2024).
114. Jones, T. et al. Early results from GLASS-JWST. XXI. Rapid asembly of a galaxy at $z$ = 6.23 revealed by its C/O abundance. *Astrophys. J. Lett.* **951**, L17 (2023).
115. Senchyna, P., Plat, A., Stark, D. P. & Rudie, G. C. GN-z11 in context: possible signatures of globular cluster precursors at redshift 10. *Astrophys. J.* **966**, 92 (2024).
116. Atek, H. et al. Most of the photons that reionized the universe came from dwarf galaxies. *Nature* **626**, 975–978 (2024).
117. Maseda, M. V. et al. JWST/NIRSpec measurements of extremely low metallicities in high equivalent width Lyα emitters. *Astrophys. J.* **956**, 11 (2023).
118. Vanzella, E. et al. An extremely metal-poor star complex in the reionization era: approaching population III stars with JWST. *Astron. Astrophys.* **678**, A173 (2023).
119. Cullen, F. et al. The ultraviolet continuum slopes ($\beta$) of galaxies at $z$ = 8–16 from JWST and ground-based near-infrared imaging. *Mon. Not. R. Astron. Soc.* **520**, 14–23 (2023).
120. Roberts-Borsani, G. et al. Between the extremes: a JWST spectroscopic benchmark for high-redshift galaxies using ~ 500 confirmed sources at $z \geqslant 5$. *Astrophys. J.* **976**, 193 (2024).
121. Shapley, A. E., Sanders, R. L., Reddy, N. A., Topping, M. W. & Brammer, G. B. JWST/NIRSpec Balmer-line measurements of star formation and dust attenuation at z ~ 3–6. *Astrophys. J.* **954**, 157 (2023).

122. Sandles, L. et al. JADES: Balmer decrement measurements at redshifts 4 < *z* < 7. *Astron. Astrophys.* **691**, A305 (2024).
123. Kokorev, V. et al. JWST insight into a lensed HST-dark galaxy and its quiescent companion at *z* = 2.58. *Astrophys. J. Lett.* **945**, L25 (2023).
124. Pérez-González, P. G. et al. CEERS key paper. IV. A triality in the nature of HST-dark galaxies. *Astrophys. J. Lett.* **946**, L16 (2023).
125. Witstok, J. et al. Carbonaceous dust grains seen in the first billion years of cosmic time. *Nature* **621**, 267–270 (2023).
126. Markov, V. et al. The evolution of dust attenuation in *z* ~ 2–12 galaxies observed by JWST. *Nat. Astron.* **9**, 458–468 (2025).
127. Herard-Demanche, T. et al. Mapping dusty galaxy growth at *z* > 5 with FRESCO: detection of Hα in submm galaxy HDF850.1 and the surrounding overdense structures. *Mon. Not. R. Astron. Soc.* **537**, 788–808 (2025).
128. Kashino, D. et al. EIGER. I. A large sample of [O III]-emitting galaxies at 5.3 < *z* < 6.9 and direct evidence for local reionization by galaxies. *Astrophys. J.* **950**, 66 (2023).
129. Wang, F. et al. A Spectroscopic Survey of Biased Halos in the Reionization Era (ASPIRE): JWST reveals a filamentary structure around a *z* = 6.61 quasar. *Astrophys. J. Lett.* **951**, L4 (2023).
130. Eilers, A.-C. et al. EIGER VI. The correlation function, host halo mass and duty cycle of luminous quasars at $z \gtrsim 6$. *Astrophys. J.* **974**, 275 (2024).
131. Helton, J. M. et al. The JWST Advanced Deep Extragalactic Survey: discovery of an extreme galaxy overdensity at *z* = 5.4 with JWST/NIRCam in GOODS-S. *Astrophys. J.* **962**, 124 (2024).
132. Onoue, M. et al. A candidate for the least-massive black hole in the first 1.1 billion years of the Universe. *Astrophys. J. Lett.* **942**, L17 (2023).
133. Barro, G. et al. Extremely red galaxies at *z* = 5–9 with MIRI and NIRSpec: dusty galaxies or obscured active galactic nuclei? *Astrophys. J.* **963**, 128 (2024).
134. Labbe, I. et al. UNCOVER: candidate red active galactic nuclei at 3 < *z* < 7 with JWST and ALMA. *Astrophys. J.* **978**, 92 (2025).
135. Kokorev, V. et al. A census of photometrically selected Little Red Dots at 4 < *z* < 9 in JWST blank fields. *Astrophys. J.* **968**, 38 (2024).
136. Kocevski, D. D. et al. Hidden little monsters: spectroscopic identification of low-mass, broad-line AGNs at *z* > 5 with CEERS. *Astrophys. J. Lett.* **954**, L4 (2023).
137. Übler, H. et al. GA-NIFS: JWST discovers an offset AGN 740 million years after the Big Bang. *Mon. Not. R. Astron. Soc.* **531**, 355–365 (2024).
138. Matthee, J. et al. Little Red Dots: an abundant population of faint active galactic nuclei at *z* ~ 5 revealed by the EIGER and FRESCO JWST surveys. *Astrophys. J.* **963**, L129 (2024).
139. Maiolino, R. et al. JADES. The diverse population of infant black holes at 4 < *z* < 11: merging, tiny, poor, but mighty. *Astron. Astrophys.* **691**, A145 (2024).
140. Greene, J. E. et al. UNCOVER spectroscopy confirms a surprising ubiquity of active galactic nuclei in red galaxies at *z* > 5. *Astrophys. J.* **964**, 39 (2024).
141. Übler, H. et al. GA-NIFS: a massive black hole in a low-metallicity AGN at *z* ~ 5.55 revealed by JWST/NIRSpec IFS. *Astron. Astrophys.* **677**, A145 (2023).
142. Scholtz, J. et al. JADES: a large population of obscured, narrow-line active galactic nuclei at high redshift. *Astron. Astrophys.* **697**, A175 (2025).
143. Yue, M. et al. Stacking X-ray observations of 'Little Red Dots': implications for their active galactic nucleus properties. *Astrophys. J. Lett.* **974**, L26 (2024).
144. Ananna, T. T., Bogdán, Á., Kovács, O. E., Natarajan, P. & Hickox, R. C. X-ray view of Little Red Dots: do they host supermassive black holes? *Astrophys. J. Lett.* **969**, L18 (2024).
145. Maiolino, R. et al. JWST meets Chandra: a large population of Compton thick, feedback-free, and intrinsically X-ray weak AGN, with a sprinkle of SNe. *Mon. Not. R. Astron. Soc.* **538**, 1921–1943 (2025).
146. Habouzit, M. Is the JWST detecting too many AGN candidates? *Mon. Not. R. Astron. Soc.* **537**, 2323–2333 (2025).
147. Harikane, Y. et al. A JWST/NIRSpec first census of broad-line AGNs at *z* = 4–7: detection of 10 faint AGNs with $M_{BH}$ $10^6$–$10^8$ $M_{\odot}$ and their host galaxy properties. *Astrophys. J.* **959**, 39 (2023).
148. Yang, J. et al. A Spectroscopic Survey of Biased Halos in the Reionization Era (ASPIRE): a first look at the rest-frame optical spectra of *z* > 6.5 quasars using JWST. *Astrophys. J. Lett.* **951**, L5 (2023).
149. Marshall, M. A. et al. GA-NIFS: black hole and host galaxy properties of two *z* = 6.8 quasars from the NIRSpec IFU. *Astron. Astrophys.* **678**, A191 (2023).
150. Bosman, S. E. I. et al. A mature quasar at cosmic dawn revealed by JWST rest-frame infrared spectroscopy. *Nat. Astron.* **8**, 1054–1065 (2024).
151. Loiacono, F. et al. A quasar–galaxy merger at *z* ~ 6.2: black hole mass and quasar properties from the NIRSpec spectrum. *Astron. Astrophys.* **685**, A121 (2024).
152. Ding, X. et al. Detection of stellar light from quasar host galaxies at redshifts above 6. *Nature* **621**, 51–55 (2023).
153. Stone, M. A., Lyu, J., Rieke, G. H., Alberts, S. & Hainline, K. N. Undermassive host galaxies of five *z* ~ 6 luminous quasars detected with JWST. *Astrophys. J.* **964**, 90 (2024).
154. Yue, M. et al. EIGER V. Characterizing the host galaxies of luminous quasars at $z \gtrsim 6$. *Astrophys. J.* **966**, 176 (2024).
155. Kokorev, V. et al. UNCOVER: a NIRSpec identification of a broad-line AGN at *z* = 8.50. *Astrophys. J. Lett.* **957**, L7 (2023).
156. Juodžbalis, I. et al. A dormant overmassive black hole in the early Universe. *Nature* **636**, 594–597 (2024).
157. Wylezalek, D. et al. First results from the JWST Early Release Science Program Q3D: turbulent times in the life of a *z* ~ 3 extremely red quasar revealed by NIRSpec IFU. *Astrophys. J. Lett.* **940**, L7 (2022).
158. Inayoshi, K., Onoue, M., Sugahara, Y., Inoue, A. K. & Ho, L. C. The age of discovery with the James Webb Space Telescope: excavating the spectral signatures of the first massive black holes. *Astrophys. J. Lett.* **931**, L25 (2022).
159. Schneider, R. et al. Are we surprised to find SMBHs with JWST at *z* ≥ 9? *Mon. Not. R. Astron. Soc.* **526**, 3250–3261 (2023).
160. Bennett, J. S., Sijacki, D., Costa, T., Laporte, N. & Witten, C. The growth of the gargantuan black holes powering high-redshift quasars and their impact on the formation of early galaxies and protoclusters. *Mon. Not. R. Astron. Soc.* **527**, 1033–1054 (2024).
161. Perna, M. et al. GA-NIFS: the ultra-dense, interacting environment of a dual AGN at *z* ~ 3.3 revealed by JWST/NIRSpec IFS. *Astron. Astrophys.* **679**, A89 (2023).
162. Ishikawa, Y. et al. VODKA-JWST: synchronized growth of two supermassive black holes in a massive gas disk? A 3.8 kpc separation dual quasar at cosmic noon with the NIRSpec Integral Field Unit. *Astrophys. J.* **982**, 22 (2025).
163. Prieto-Lyon, G. et al. The production of ionizing photons in UV-faint *z* ~ 3–7 galaxies. *Astron. Astrophys.* **672**, A186 (2023).
164. Simmonds, C. et al. The ionizing photon production efficiency at *z* ~ 6 for Lyman-alpha emitters using JEMS and MUSE. *Mon. Not. R. Astron. Soc.* **523**, 5468–5486 (2023).
165. Dayal, P. et al. UNCOVERing the contribution of black holes to reionization. *Astron. Astrophys.* **697**, A211 (2025).
166. Mascia, S. et al. Closing in on the sources of cosmic reionization: first results from the GLASS-JWST program. *Astron. Astrophys.* **672**, A155 (2023).

167. Lin, Y.-H. et al. An empirical reionization history model inferred from the low-redshift Lyman continuum survey and the star-forming galaxies at $z > 8$. *Mon. Not. R. Astron. Soc.* **527**, 4173–4182 (2024).
168. Nakane, M. et al. Lyα emission at $z = 7$–13: clear evolution of Lyα equivalent width indicating the late cosmic reionization history. *Astrophys. J.* **967**, 28 (2024).
169. Chen, Y., Mo, H. J. & Wang, K. Massive dark matter haloes at high redshift: implications for observations in the JWST era. *Mon. Not. R. Astron. Soc.* **526**, 2542–2559 (2023).
170. Umeda, H. et al. JWST measurements of neutral hydrogen fractions and ionized bubble sizes at $z = 7$–12 obtained with Lyα damping wing absorptions in 27 bright continuum galaxies. *Astrophys. J.* **971**, 124 (2024).
171. Morishita, T. et al. Early results from GLASS-JWST. XIV. A spectroscopically confirmed protocluster 650 million years after the Big Bang. *Astrophys. J. Lett.* **947**, L24 (2023).
172. Chen, Z. et al. JWST spectroscopy of $z \sim 5$–8 UV-selected galaxies: new constraints on the evolution of the Ly α escape fraction in the reionization era. *Mon. Not. R. Astron. Soc.* **528**, 7052–7075 (2024).
173. Napolitano, L. et al. Peering into cosmic reionization: the Lyα visibility evolution from galaxies at $z = 4.5$–8.5 with JWST. *Astron. Astrophys.* **688**, A106 (2024).
174. Heintz, K. E. et al. Strong damped Lyman-α absorption in young star-forming galaxies at redshifts 9 to 11. *Science* **384**, 890–894 (2024).
175. Lu, T.-Y. et al. The reionizing bubble size distribution around galaxies. *Mon. Not. R. Astron. Soc.* **528**, 4872–4890 (2024).
176. Saxena, A. et al. JADES: the production and escape of ionizing photons from faint Lyman-alpha emitters in the epoch of reionization. *Astron. Astrophys.* **684**, A84 (2024).
177. Tang, M. et al. Lyα emission in galaxies at $z \simeq 5$–6: new insight from JWST into the statistical distributions of Lyα properties at the end of reionization. *Mon. Not. R. Astron. Soc.* **531**, 2701–2730 (2024).
178. Witstok, J. et al. Inside the bubble: exploring the environments of reionisation-era Lyman-α emitting galaxies with JADES and FRESCO. *Astron. Astrophys.* **682**, A40 (2024).
179. Meyer, R. A. et al. JWST FRESCO: a comprehensive census of Hβ + [O III] emitters at $6.8 < z < 9.0$ in the GOODS fields. *Mon. Not. R. Astron. Soc.* **535**, 1067–1094 (2024).
180. Álvarez-Márquez, J. et al. Spatially resolved Hα and ionizing photon production efficiency in the lensed galaxy MACS1149–JD1 at a redshift of 9.11. *Astron. Astrophys.* **686**, A85 (2024).
181. Welch, B. et al. JWST imaging of Earendel, the extremely magnified star at redshift $z = 6.2$. *Astrophys. J. Lett.* **940**, L1 (2022).

## Acknowledgements

While this Perspective is written by a small number of authors, invited to ISSI Bern in March 2024 as part of the 2024 ISSI Breakthrough Workshop, we acknowledge the work of a large community that is advancing our collective understanding of the evolution of the early Universe. We thank ISSI for sponsoring the 2024 Breakthrough Workshop, and the ISSI staff for their wonderful welcome and support. We are grateful to the author collaborators, who made this paper possible. Collectively, we are grateful to the large group of committed scientists and engineers, worldwide, who designed, built and commissioned the JWST and made a decades-long astronomer dream a reality. R.P.N. is a NASA Hubble Fellow. We are grateful to M. Dickinson for a careful read of the final paper and to F. Crameri (ISSI) for his expert help designing the very best figures. We dedicate this paper to the 20,000 people who spent decades to make JWST an incredible discovery machine.

## Author contributions

All of the authors were invited participants at a breakthrough workshop at the International Space Science Institute, titled 'The chronology of the very early Universe according to JWST', which was held on 11–15 March 2024, in Bern, Switzerland. Most participants were successful JWST Cycle 1 principal investigators of medium and large cosmology programmes. All authors actively participated in workshop discussions and writing of the paper. The conveners of the workshop were A.N., A.A., G.B., D.C., P.A.O. and J.R.R. The editors were the conveners and D.J.E. The leads of the individual sections of the paper were P.A.O., D.C., A.A., R.B., D.J.E., A.F., M.H., R.M., C.M., A.E.S. and M.S. The discussion moderators were J.R.R., D.A.B., J.C., P.D., I.L., M.V.M., J.M., K.B.W.M., D.S., A.L.S., C.C.W. and D.W. The discussion notetakers were G.B., A.d.G., T.A.H., J.S.K., R.M.-C. and R.P.N. G.R.-B. analysed the data and produced Figs. 2 and 4.

## Competing interests

The authors declare no competing interests.

## Additional information

**Correspondence** should be addressed to Antonella Nota.

**Peer review information** *Nature Astronomy* thanks Karl Glazebrook and the other, anonymous, reviewer(s) for their contribution to the peer review of this work.



[1]Department of Astronomy, The Oskar Klein Centre, Stockholm University, AlbaNova, Stockholm, Sweden. [2]Institut d'Astrophysique de Paris, CNRS, Sorbonne Université, Paris, France. [3]Department of Astronomy, The University of Texas at Austin, Austin, TX, USA. [4]Max Planck Institut für Astronomie, Heidelberg, Germany. [5]Department of Astronomy, University of Illinois at Urbana-Champaign, Urbana, IL, USA. [6]Department of Physics and Astronomy and PITT PACC, University of Pittsburgh, Pittsburgh, PA, USA. [7]University of Ljubljana, Faculty of Mathematics and Physics, Ljubljana, Slovenia. [8]Department of Physics and Astronomy, University of California Davis, Davis, CA, USA. [9]Cosmic Dawn Center (DAWN), Copenhagen, Denmark. [10]Niels Bohr Institute, University of Copenhagen, Copenhagen, Denmark. [11]Institute for Astronomy, University of Edinburgh, Edinburgh, UK. [12]Space Telescope Science Institute, Baltimore, MD, USA. [13]Association of Universities for Research in Astronomy (AURA), Inc. for the European Space Agency (ESA), STScI, Baltimore, MD, USA. [14]Department of Physics and Astronomy, The Johns Hopkins University, Baltimore, MD, USA. [15]Kapteyn Astronomical Institute, University of Groningen, Groningen, The Netherlands. [16]Center for Astrophysics | Harvard & Smithsonian, Cambridge, MA, USA. [17]Department of Physics, University of Auckland, Auckland, New Zealand. [18]Scuola Normale Superiore, Pisa, Italy. [19]Astrophysics Science Division, Code 660, NASA Goddard Space Flight Center, Greenbelt, MD, USA. [20]Laboratory for Multiwavelength Astrophysics, School of Physics and Astronomy, Rochester Institute of Technology, Rochester, NY, USA. [21]Leiden Observatory, Leiden University, Leiden, The Netherlands. [22]Centre for Astrophysics

and Supercomputing, Swinburne University of Technology, Melbourne, Victoria, Australia. [23]Kavli Institute for Cosmology, University of Cambridge, Cambridge, UK. [24]Cavendish Laboratory - Astrophysics Group, University of Cambridge, Cambridge, UK. [25]Department of Physics and Astronomy, University College London, London, UK. [26]Department of Astronomy, University of Geneva, Versoix, Switzerland. [27]Department of Astronomy, University of Wisconsin-Madison, Madison, WI, USA. [28]Institute of Science and Technology Austria (ISTA), Klosterneuburg, Austria. [29]Department of Physics and Astronomy, Rutgers, the State University of New Jersey, Piscataway, NJ, USA. [30]MIT Kavli Institute for Astrophysics and Space Research, Cambridge, MA, USA. [31]INAF –OAR Osservatorio Astronomico di Roma, Monte Porzio Catone, Italy. [32]Centro de Astrobiología (CAB), CSIC-INTA, Torrejón de Ardoz, Madrid, Spain. [33]Department of Physics and Astronomy, University of California Los Angeles, Los Angeles, CA, USA. [34]Department of Astronomy, University of Arizona, Tucson, AZ, USA. [35]Center for Interdisciplinary Exploration and Research in Astrophysics (CIERA), Northwestern University, Evanston, IL, USA. [36]Department of Physics and Astronomy, Northwestern University, Evanston, IL, USA. [37]INAF – OAS, Osservatorio di Astrofisica e Scienza dello Spazio di Bologna, Bologna, Italy. [38]Steward Observatory, University of Arizona, Tucson, AZ, USA. [39]Department of Astronomy, University of Michigan, Ann Arbor, MI, USA. [40]Astronomy Centre, University of Sussex, Falmer, UK. [41]Institute of Space Sciences and Astronomy, University of Malta, Msida, Malta. [42]NSF's National Optical-Infrared Astronomy Research Laboratory, Tucson, AZ, USA. [43]NRC Herzberg, Victoria, British Columbia, Canada. [44]Astronomisches Rechen-Institut, Zentrum für Astronomie der Universität Heidelberg, Heidelberg, Germany. [45]International Space Science Institute, Bern, Switzerland. ✉e-mail: antonella.nota@issibern.ch